

# Nuclear response using correlated realistic interactions: first-order random phase approximation and beyond\*

P. Papakonstantinou<sup>a</sup>, R. Roth<sup>a</sup> and N. Paar<sup>ab</sup>

<sup>a</sup>Institut für Kernphysik, Technische Universität Darmstadt, Schlossgartenstr. 9, D-64289 Darmstadt, Germany

<sup>b</sup>Physics Department, Faculty of Science, University of Zagreb, Croatia

A correlated realistic interaction derived within the Unitary Correlation Operator Method (UCOM) based on the Argonne V18 nucleon-nucleon potential is used in calculations of nuclear response for closed-shell nuclei. Giant resonances are examined in the framework of the random-phase approximation (RPA). The effects of explicit ground-state correlations and of higher than first-order configurations are discussed.

## 1. INTRODUCTION

Nowadays, highly accurate parameterizations of the bare nucleon-nucleon (NN) force have become available [1–3]. At the same time, attempts are being made to derive the two-, three-, and many-nucleon force from first principles, within chiral perturbation theory [4,5]. The possibility is being explored to combine mean-field theory with realistic NN potentials. Two methods have been developed recently for regulating the NN interaction for implementation within models like Hartree-Fock (HF) and random-phase approximation (RPA): a low-momentum interaction, the  $V_{\text{low-}k}$ , is derived within renormalization group theory [6]; a correlated NN interaction, the  $V_{\text{UCOM}}$ , is derived using the Unitary Correlation Operator Method (UCOM) [7–9]. Although constructed following different formalisms, the two potentials have similar low-momentum matrix elements. In this work we focus on the UCOM potential.

Within the UCOM, the major short-range correlations, induced by the strong repulsive core and the tensor part of the bare NN potential, are described by a state-independent unitary correlation operator. This can be used to introduce correlations into an uncorrelated many-body state or, alternatively, to perform a similarity transformation of an operator of interest. Applied to a realistic NN interaction, the method produces a “correlated” interaction,  $V_{\text{UCOM}}$ , which is phase-shift equivalent to the bare one and which can be used as a universal effective interaction, for calculations within simple Hilbert spaces.

The utilization of the UCOM involves a cluster expansion of the correlated operators and, currently, a truncation at the two-body level. The latter is justified by the short range of the correlations treated by the method. The correlation functions are determined by minimizing the energy of the two-nucleon system. The only free parameter that remains is

---

\*Work supported by the Deutsche Forschungsgemeinschaft under contract SFB 634

the range of the tensor correlations, which is restricted in order to mimic the screening of the tensor interaction between nucleons embedded in many-nucleon systems. It turns out that for an appropriate choice of this parameter the contributions of the missing genuine three-body force and the omitted terms of the cluster expansion effectively cancel each other, at least as far as the binding energies of nuclei are concerned [10–12]. The same does not necessarily hold, however, for other ground-state observables, such as charge radii, or for excited-state properties.

The aim of the UCOM is to treat explicitly only the state-independent short-range correlations; long-range correlations should be described by the model space. Since a Slater-determinant wave function is unable to describe correlations, the UCOM-based HF can not be sufficient for a description of bulk nuclear properties in finite nuclei. It was found indeed that, although bound nuclei were obtained using the  $V_{\text{UCOM}}$  already at the HF level, the binding energies were underestimated by about 4 MeV per nucleon [11]. Second-order perturbation theory, however, constitutes a tractable and adequate extension to the “zero-order” description provided by HF, as far as nuclear binding energies are concerned [11].

In this work we discuss the performance of the  $V_{\text{UCOM}}$  in describing nuclear collective excitations in the framework of RPA. We study closed-shell nuclei across the nuclear chart by employing (i) a standard, self-consistent first-order RPA, where the ground state is approximated with the uncorrelated HF state, (ii) a renormalized version [13–15], built on the true RPA ground state, which allows us to take into account the Fermi sea depletion, and which we will call Extended RPA (ERPA) following Ref. [15], and (iii) a second-order version (SRPA) [16,17], built on the HF ground state, where the coupling between one-particle – one-hole ( $ph$ ) and two-particle – two-hole ( $2p2h$ ) states is included, but the coupling between  $2p2h$  states is ignored for the moment. We discuss results obtained with the  $V_{\text{UCOM}}$ , derived from the Argonne V18 interaction.

In Sec. 2 we present our results. First, we summarize the results of the usual RPA, as reported in Ref. [18]. In Sec. 2.1 we examine the effect of explicit RPA correlations present in the ground state by using the ERPA, see also Ref. [19]. The limitations of first-order RPA are pointed out. Finally, in Sec. 2.2, preliminary results of second-order RPA are reported, demonstrating the important effect of the extended model space. We conclude in Sec. 3.

## 2. CORRELATED INTERACTION AND RPA

In a recent publication [18] we applied the UCOM Hamiltonian in standard, self-consistent RPA calculations to study nuclear giant resonances. The main focus was on the isoscalar (IS) giant monopole resonance (GMR), the isovector (IV) giant dipole resonance (GDR) and the IS giant quadrupole resonance (GQR). Such highly collective states were indeed obtained, for various closed-shell nuclei ranging from  $^{16}\text{O}$  to  $^{208}\text{Pb}$ . We achieved a reasonable agreement with the experimental centroid energies of the IS GMR. By contrast, the energies of the IV GDR and the IS GQR were overestimated by several MeV.

Obviously, the  $V_{\text{UCOM}}$  is not a traditional effective interaction. In part because no long-range correlations are (effectively) included in the UCOM, the corresponding nucleon effective mass in nuclear matter is very low — according to a HF calculation, less than

half the bare nucleon mass. This is verified by the HF results in finite nuclei: the single-particle level density was found too low [11]. It is also manifested by the above-mentioned RPA results on the GQR and GDR centroids. Clearly, besides the possible important role of missing three-body terms in the Hamiltonian, another source of our failure to describe nuclear collective states quantitatively can be the inadequacy of the RPA method to take into account residual long-range correlations.

The standard RPA is based on two assumptions which hint at possible remedies. First of all, only  $ph$  excitations are taken into account. One can include higher-order configurations, starting with  $2p2h$  within SRPA. Given that an extended model space is of great importance when using the  $V_{UCOM}$ , it is imperative to examine the effect. The other assumption is that one can approximate the true RPA ground state by the HF ground state without introducing great errors. One argument follows from the fact that the RPA is the theory of small-amplitude vibrations around the HF ground state, therefore correlations should be small anyway for the use of RPA to be justified. It is not obvious that this assumption holds when the UCOM Hamiltonian is used, given the large correction to the HF binding energies due to second-order [11] and RPA [12] correlations.

In the following we address both effects.

### 2.1. Extended RPA (ERPA)

Next, we will examine the effect of explicit RPA ground-state correlations on the excitation spectra for nuclear collective states. To this end we use a renormalized version of the RPA, developed in Refs. [13–15], where excited states are built on top of the true RPA ground state. The model is formulated in the single-particle basis which diagonalizes the one-body density matrix, i.e., the natural-orbital basis, and its equations are solved iteratively. We will call it Extended RPA (ERPA) following Ref. [15]. Within the ERPA, consider explicitly the depletion of the Fermi sea in the ground state due to RPA correlations. The ERPA is derived using the number-operator method, which, contrary to the quasi-boson approximation, does not suffer from double-counting the second-order contributions [15,20].

The depletion of the Fermi sea enters directly the ERPA equations and the calculation of the transition matrix elements via the quantities  $D_{ph} \equiv \rho_h - \rho_p$ , where  $\rho_i$  denotes the occupation probability of the particle ( $i = p$ ) or hole ( $i = h$ ) state. These quantities appear as prefactors weakening the residual interaction. Thus, for static single-particle states, the depletion of the Fermi sea is expected in general to push the isovector strength to lower energies and the isoscalar strength to higher energies, compared to the usual RPA. At the same time, though, the single-particle states of the correlated ground state are closer in energy to each other compared to those of the HF solution [19]. The effect of the weakening of the effective interaction should thereby be moderated in the isoscalar channel and enhanced in the isovector channel.

Our numerical results are more or less in line with the above expectations. In Fig. 1 we show the centroid energies of the IS GMR, IV GDR and IS GQR obtained for the nuclei  $^{16}\text{O}$ ,  $^{40}\text{Ca}$ ,  $^{90}\text{Zr}$ ,  $^{100}\text{Sn}$ , and  $^{208}\text{Pb}$  within the RPA (solid bars) and ERPA (dotted bars), compared with some experimental data (points). As examples, we show in Fig. 2 the corresponding IS monopole and IV dipole strength distributions for  $^{16}\text{O}$  and  $^{90}\text{Zr}$ . In all cases shown in Figs. 1, 2, except for  $^{208}\text{Pb}$ , we have used a single-particle basis of

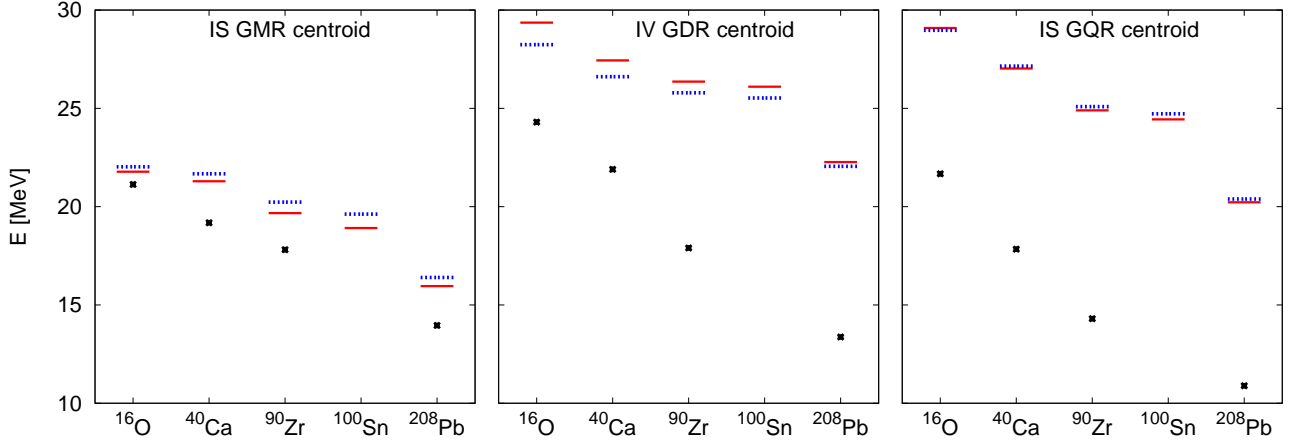


Figure 1. Centroid energies of the IS GMR, IV GDR and IS GQR obtained for the nuclei  $^{16}\text{O}$ ,  $^{40}\text{Ca}$ ,  $^{90}\text{Zr}$ ,  $^{100}\text{Sn}$ , and  $^{208}\text{Pb}$  within the RPA (solid bars) and ERPA (dotted bars), compared with experimental data (points — for references see text). In calculating the centroids, the strength up to 50 MeV was taken into account.

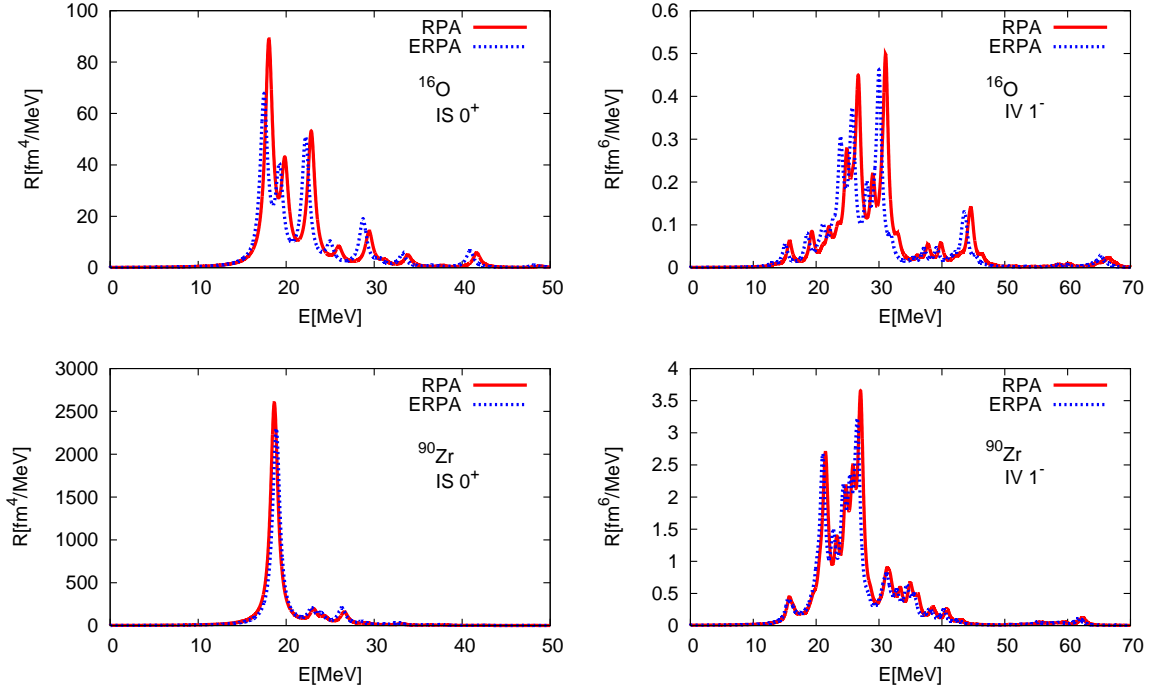


Figure 2. IS monopole and IV dipole strength distributions of  $^{16}\text{O}$  and  $^{90}\text{Zr}$  computed within RPA (red solid lines) and ERPA (blue dotted lines). The discrete strength distributions have been folded with a Lorentzian of width  $\Gamma = 2$  MeV.

13 oscillator shells and for evaluating the ground-state correlations we have taken into account states with angular momentum up to  $J_{\max} = 4$  and both parities, but without charge exchange. For  $^{208}\text{Pb}$ , a basis of 15 shells was employed to ensure convergence in this heavy nucleus and  $J_{\max} = 3$  was used to avoid an extremely time-consuming calculation. The strength distributions up to 50 MeV were taken into account when calculating the centroid energies, which are defined as the first energy moment of the distribution,  $m_1$ , divided by the total strength,  $m_0$ . The experimental centroids of the IS GMR and the IS GQR were taken from Refs. [21] ( $^{16}\text{O}$ ), [22] ( $^{40}\text{Ca}$ ), [23] ( $^{90}\text{Zr}$ ), and [24] ( $^{208}\text{Pb}$ ). Photoabsorption cross sections were found in Refs. [25] ( $^{16}\text{O}$ ), [26] ( $^{40}\text{Ca}$ ), [27] ( $^{90}\text{Zr}$ ), and [28,29] ( $^{208}\text{Pb}$ ) and the centroids  $m_1/m_0$  of the corresponding IV GDR strength distributions were evaluated from those.

We found that, for all nuclei and excitation fields examined, the total strength  $m_0$  and total energy-weighted strength  $m_1$  decrease within ERPA. The relative change remains below 10% in almost all cases, being largest for the lightest nuclei. Within ERPA the spurious dipole state is found at approximately 1 MeV, i.e., somewhat further from zero than within RPA. We should note that self consistency is slightly violated by ERPA. Although particle-particle and hole-hole transitions are allowed by the model space, these are not taken into account.

From Fig. 1 it is evident that the energy of the GDR drops when ground-state correlations are explicitly considered within the ERPA, but not enough to reach the experimental data. In general, a decrease of no more than 1 MeV was achieved for the heavier nuclei. The same holds for the IV  $0^+$  and  $2^+$  centroids (not shown). The IS giant resonances, namely the IS GMR, GDR (not shown) and GQR, were less affected. In most cases, their energies were higher when evaluated within ERPA than within RPA. Apparently, ground-state correlations alone cannot explain the discrepancy between our RPA results and experimental data.

We should mention that, as RPA calculations of ground-state energies suggest [12], in order to achieve good convergence when describing RPA correlations one may need to take into account  $J_{\max}$  values up to approximately 10. For ERPA, such large values are beyond our computational capabilities at present. Since, however, no strongly collective states with multipolarities larger than 4 are expected, and based also on the results of Ref. [12], it is reasonable to speculate that the difference between the RPA and ERPA results would be no more than doubled if higher values of  $J_{\max}$  were considered. Of course, no charge-exchange excitations have been taken into account here. These can introduce additional correlations of non-negligible amplitude, albeit smaller than the non-exchange ones [12].

## 2.2. Second-order RPA (SRPA)

Next we employ a simple SRPA model, where the ground state is described by the HF model and the coupling between  $2p2h$  states is not taken into account. Therefore, the results presented here should be considered preliminary.

In Fig. 3 we show the IV dipole and IS quadrupole strength distributions of the nucleus  $^{40}\text{Ca}$  as calculated within the usual, first-order RPA and within the SRPA. We have truncated the  $2p2h$  space by allowing only states with energy  $E_{2p2h}$  up to a maximal value, which we have varied. We observe that the coupling of the  $ph$  states to  $2p2h$

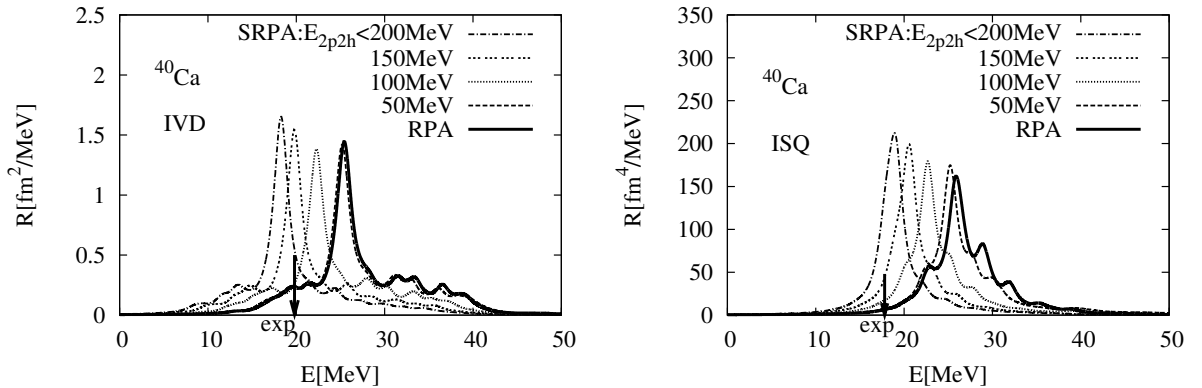


Figure 3. IV dipole and IS quadrupole strength distributions of  $^{40}\text{Ca}$  within SRPA for various values of the  $2p2h$ -space truncation energy and within first-order RPA.

excitations has the effect of pushing the strength to lower energies, as expected [30]. The effect is strong enough to lower the centroid energies of the giant resonances down to the experimental values, indicated by arrows on the figures. Convergence with respect to the truncation energy has not been reached yet. Further calculations are planned, for more nuclei and larger  $2p2h$  bases. The coupling within the  $2p2h$  space should also be included in future calculations.

### 3. SUMMARY

We have employed the correlated Argonne V18 two-body interaction, derived within the UCOM, in RPA calculations of nuclear collective excitations. We found that first-order RPA could not reproduce the quantitative features of some giant resonances, even after ground-state correlations are explicitly taken into account. SRPA, though, yielded promising results in preliminary calculations. More comprehensive studies are going to be performed in the near future. Other excited states will be investigated as well, in particular spin-flip and charge-exchange ones. We are also planning to include three-body effects via a simple phenomenological three-body term in the interaction.

### REFERENCES

1. R. Wiringa, V. Stoks, R. Schiavilla, Phys. Rev. C51 (1995) 38.
2. R. Machleidt, Phys. Rev. C63 (2001) 024001.
3. V. Stoks, R. Klomp, C. Terheggen, J. de Swart, Phys. Rev. C49 (1994) 2950.
4. D. Entem, R. Machleidt, Phys. Rev. C68 (2003) 041001.
5. E. Epelbaum, W. Glöckle, U.-G. Meißner, Nucl. Phys. A747 (2005) 362.
6. S. Bogner, T. Kuo, A. Schwenk, Phys. Rep. 386 (2003) 1.
7. H. Feldmeier, T. Neff, R. Roth, J. Schnack, Nucl. Phys. A632 (1998) 61.
8. T. Neff, H. Feldmeier, Nucl. Phys. A713 (2003) 311.
9. R. Roth, T. Neff, H. Hergert, H. Feldmeier, Nucl. Phys. A745 (2004) 3.

10. R. Roth, H. Hergert, P. Papakonstantinou, T. Neff, H. Feldmeier, Phys. Rev. C72 (2005) 034002.
11. R. Roth, P. Papakonstantinou, N. Paar, H. Hergert, T. Neff, H. Feldmeier, Phys. Rev. C73 (2006) 044312.
12. C. Barbieri, N. Paar, R. Roth, P. Papakonstantinou, Phys. Rev. Lett. submitted, nucl-th/0608011.
13. F. Catara, G. Piccitto, M. Sambataro, N. Van Giai, Phys. Rev. B54 (1996) 17536.
14. F. Catara, M. Grasso, G. Piccitto, M. Sambataro, Phys. Rev. B58 (1998) 16070.
15. V. Voronov, D. Karadjov, F. Catara, A. Severyukhin, Phys. Part. Nucl. 31 (2000) 904.
16. C. Yannouleas, Phys. Rev. C35 (1987) 1159.
17. S. Drożdż, S. Nishizaki, J. Speth, J. Wambach, Phys. Rep. 197 (1990) 1.
18. N. Paar, P. Papakonstantinou, H. Hergert, R. Roth, Phys. Rev. C74 (2006) 014318.
19. P. Papakonstantinou, R. Roth, N. Paar, Phys. Rev. C submitted, nucl-th/0609039.
20. D. J. Rowe, Phys. Rev. 175 (1968) 1283.
21. Y.-W. Lui, H. Clark, D. Youngblood, Phys. Rev. C64 (2001) 064308.
22. D. Youngblood, Y.-W. Lui, H. Clark, Phys. Rev. C63 (2001) 067301.
23. D. Youngblood, Y.-W. Lui, B. John, Y. Tokimoto, H. Clark, X. Chen, Phys. Rev. C69 (2004) 054312.
24. D. Youngblood, Y.-W. Lui, H. Clark, Y. Tokimoto, X. Chen, Phys. Rev. C69 (2004) 034315.
25. S. LeBrun, A. Nathan, S. Hoblit, Phys. Rev. C35 (1987) 2005.
26. A. Veyssi re, H. Beil, R. Berg re, P. Carlos, A. Lepr tre, A. de Miniac, Nucl. Phys. A227 (1974) 513.
27. B. Berman, J. Caldwell, R. Harvey, M. Kelly, R. Bramblett, S. Fultz, Phys. Rev. 162 (1967) 1098.
28. A. Veyssi re, H. Beil, R. Berg re, P. Carlos, A. Lepr tre, Nucl. Phys. A159 (1970) 561.
29. B. Berman, S. Fultz, Rev. Mod. Phys. 47 (1975) 713.
30. J. Wambach, Rep. Prog. Phys. 51 (1988) 989.